THE JOURNAL OF BIOLOGICAL CHEMISTRY VOL. 284, NO. 14, pp. 9247–9256, April 3, 2009

Distinct Transport and Intracellular Activities of Two GlcAT-P Isoforms*[S]

Received for publication, September 29, 2008, and in revised form, December 17, 2008 Published, JBC Papers in Press, January 30, 2009, DOI 10.1074/jbc.M807517200

Yasuhiko Kizuka[‡], **Yasuhiro Tonoyama**[§], **and Shogo Oka**[§1]

From the [‡]*Department of Biological Chemistry, Graduate School of Pharmaceutical Sciences, and the* [§]*Department of Biological Chemistry, Human Health Sciences, Graduate School of Medicine, Kyoto University, Kyoto 606-8507, Japan*

A neural glycotope, human natural killer-1 carbohydrate, is involved in synaptic plasticity. The key biosynthetic enzyme is a glucuronyltransferase, GlcAT-P, a type II membrane protein comprising an N-terminal cytoplasmic tail, transmembrane domain, stem region, and C-terminal catalytic domain. Previously, we reported that GlcAT-P has two isoforms differing in only the presence or absence of the N-terminal 13 amino acids (P-N13) in the cytoplasmic tail, but the functional distinction of these two isoforms has not been reported. Herein, we show that when expressed in Neuro2A cells, short form GlcAT-P (sGlcAT-P) exhibited significantly higher glucuronylation activity than the longer form (lGlcAT-P), despite their comparable specific activities *in vitro*. In addition, sGlcAT-P was strictly localized in Golgi apparatus, whereas lGlcAT-P was mainly localized in Golgi but partly in the endoplasmic reticulum. We demonstrated that the small GTPase, Sar1, recognized a dibasic motif in the cytoplasmic tail near P-N13 that was important for exiting the endoplasmic reticulum, and Sar1 interacted with sGlcAT-P more strongly than lGlcAT-P. Finally, the attachment of P-N13 to another glycosyltransferase, polysialyltransferase-I (ST8Sia-IV), had similar effects, such as reduced activity and entrapment within endoplasmic reticulum. These results suggest that P-N13 can control glycosyltransferase transport through Sar1 binding interference.

A number of reports have revealed that glycosylation plays diverse roles in many biological events, such as development and disease progression (1). During glycan biosynthesis, ER-[2] and Golgi-resident glycosyltransferases catalyze reactions in a stepwise manner to construct diverse glycoconjugates (2). Among glycan epitopes (glycotopes), we have been investigating the functions of human natural killer-1 (HNK-1) carbohydrate, which is highly expressed on several cell adhesion molecules in the nervous system (3). This carbohydrate epitope, comprising a unique trisaccharide structure, HSO_3-3GlcAβ1–3Galβ1–4GlcNAc-, is sequentially biosynthesized by one of two glucuronyltranferases (GlcAT-P and GlcAT-S) and by a specific sulfotransferase (HNK-1ST) (4–6). We generated and analyzed GlcAT-P gene-deficient mice and revealed that the marked loss of the HNK-1 carbohydrate in the nervous system caused the impairment of hippocampal synaptic plasticity, learning, and memory (7). These results indicated that GlcAT-P is the main HNK-1-synthesizing enzyme in the brain and that this carbohydrate is important to maintain proper neural function. Therefore, elucidation of the regulatory mechanism for the HNK-1 biosynthesis will lead to the clarification of how this carbohydrate controls neural function. Recently, we reported that an enzyme complex consisting of GlcAT-P (or GlcAT-S) and HNK-1ST positively regulates the efficiency of HNK-1 biosynthesis (8). In addition, it was reported that other glycosyltransferases and glycosylation-related proteins were associated in cells to regulate glycoconjugate biosynthesis (9). Therefore, it is evident that not only the expression of a glycosyltransferase but also its regulation mechanism, including enzyme complex formation, is indispensable to understand the overall glycosylation system *in vivo*.

Most glycosyltransferases are commonly type II membrane proteins, comprising a short N-terminal cytoplasmic tail, transmembrane domain, stem region, and large C-terminal catalytic domain (10). Most of them reside at a specific location in the Golgi apparatus (11), where specific glycosylation occurs. The currently supported concept is that the region comprising the N-terminal cytoplasmic tail to the stem domain is sufficient for the Golgi retention of glycosyltransferase and that the C-terminal domain is responsible for the catalytic reaction. In fact, some chimeric enzymes consisting of an N-terminal region (from the N terminus to stem) fused with a fluorescent protein like green fluorescent protein exhibited appropriate localization in the Golgi apparatus (12), whereas recombinant soluble catalytic domains showed enzymatic activities with high substrate specificities *in vitro* (13). In recent years, however, a growing number of findings have revealed that the N-terminal cytoplasmic tail of glycosyltransferases plays various roles in cells. For instance, β1,4-galactosyltransferase-I (B4GalT-I) has two forms differing in their cytoplasmic tail length, and it was shown that the longer form was localized both in the Golgi apparatus and on the cell surface, whereas the

* This work was supported in part by Grant-in-Aid for Creative Scientific Research 16GS0313 (to S. O.) and a Grant-in-Aid for JSPS Fellows (to Y. K.) from the Ministry of Education, Culture, Sports, Science, and Technology. The costs of publication of this article were defrayed in part by the payment of page charges. This article must therefore be hereby marked "*advertisement*" in accordance with 18 U.S.C. Section 1734 solely to indicate this fact.

[S] The on-line version of this article (available at http://www.jbc.org) contains supplemental Fig. 1.

[1] To whom correspondence should be addressed: Kawahara-cho 53, Shogoin, Sakyo-ku, Kyoto 606-8507, Japan. Tel./Fax: 81-75-751-3959; E-mail: shogo@hs.med.kyoto-u.ac.jp.

[2] The abbreviations used are: ER, endoplasmic reticulum; B4GalT-I, β1,4-galactosyltransferase-I; GlcAT, glucuronyltransferase; G-N13, N-terminal 13 amino acids of long form B4GalT-I; HNK-1, human natural killer-1; lGlcAT-P, long form GlcAT-P; P-N13, N-terminal 13 amino acids of lGlcAT-P; PNGase F, peptide:*N*-glycosidase F; PSA, polysialic acid; PST, polysialyltransferase-I; sGlcAT-P, short form GlcAT-P; ST6Gal-I, β-galactoside α2,6-sialyltransferase-I; mAb, monoclonal antibody; pAb, polyclonal antibody.

shorter form resided only in the Golgi (14), and that the cycling between the *trans*-Golgi cisterna and the *trans*-Golgi network was mediated by a signal contained in the longer cytoplasmic tail (15). Maccioni's group (16) reported that the basic amino acid motifs commonly found in the cytoplasmic tails of some glycosyltransferases were required for their exit from ER to the Golgi apparatus. More recently, it was reported that Vps74p recognized and bound to the cytoplasmic tails of many glycosyltransferases and functioned to retain them in the Golgi apparatus in yeast (17, 18). These reports underscore the importance of the cytoplasmic tail of glycosyltransferases, especially for their appropriate localization in cells.

Previously, we reported that GlcAT-P mRNA has two alternative splicing variants in mouse, rat, and human brains (19, 20). A 16-bp insertion was found soon after the initiation codon in the longer mRNA in mice (20), and a similar 17-bp insertion was found in humans (19) (Fig. 1*A*). Since the insertion created a new stop codon in frame, the second ATG (Fig. 1*A*, *underlined*) was probably used as an alternative initiation codon. As a result, the longer mRNA was translated into a shorter protein. Therefore, the alternative splicing generates the long and short forms of the enzyme, and these two isoforms are considered to be identical except for the additional N-terminal 13 amino acids in the cytoplasmic tail (Fig. 1*B*, lGlcAT-P and sGlcAT-P). However, no functional difference between these two isoforms has yet been clarified. In this study, we found significant differences in intracellular activity and localization between the two isoforms, probably caused by the distinct rate of export from ER. These data suggest a unique Golgi localization mechanism of GlcAT-P involving the cytoplasmic tail.

EXPERIMENTAL PROCEDURES

Materials—Monoclonal antibody (mAb) M6749 was a generous gift from Dr. H. Tanaka (Kumamoto University). Mouse anti-FLAG M2 mAb was purchased from Sigma. Rabbit anti-GlcAT-P pAb (GP2) was raised in a rabbit against the recombinant human GlcAT-P catalytic region expressed and purified from *Escherichia coli*. Rabbit anti-P-N13 (corresponding to the N-terminal 13 amino acids of lGlcAT-P) pAb was raised against a synthetic peptide (MGNEELWAQPALE). Mouse anti-PSA mAb (12E3) was kindly provided by Dr. T. Seki (Juntendo University). Mouse anti-T7 mAb was purchased from Novagen (Madison, WI). Mouse anti-GM130 mAb was purchased from BD Biosciences. Rabbit anti-human IgG-Fc pAb was from Jackson ImmunoResearch Laboratories (West Grove, PA). Biotinylated wheat germ agglutinin was from Seikagaku Corp. (Tokyo, Japan). Horseradish peroxidase-conjugated anti-mouse IgG, anti-mouse IgM, and anti-rabbit IgG were purchased from Zymed Laboratories Inc. (South San Francisco, CA). Alexa Fluor 488-conjugated anti-rabbit IgG and Alexa Fluor 546-conjugated anti-mouse IgG were obtained from Molecular Probes, Inc. (Eugene, OR). Rhodamine-conjugated Avidin D was from Vector Laboratories (Burlingame, CA). Protein G-Sepharose TM4 Fast Flow was purchased from GE Healthcare.

Expression Plasmids—The subcloning of rat lGlcAT-P cDNA into pEF-BOS (pEF-BOS/lGlcAT-P) was performed as described previously (4). Rat sGlcAT-P cDNA (including a 16-bp (GTGGGTGTGAGCGCTG) insertion right after the initiation codon for lGlcAT-P) was subcloned into pEF-BOS (pEF-BOS/sGlcAT-P) in the same way as for pEF-BOS/lGlcAT-P. The insertion of lGlcAT-PΔstem cDNA into pEF-1/V5-His A (Invitrogen) was performed as follows. Two fragments were amplified by PCR using pEF-BOS/lGlcAT-P as a template with the two sets of primers listed below to create a 5′-EcoRI site in the shorter fragment and a 3′-NotI site in the longer fragment. After the fragments had been digested with EcoRI or NotI, respectively, the ends of both fragments were phosphorylated with polynucleotide kinase. Then the two fragments were simultaneously ligated to pEF-1/V5-His A, which had been double-digested with EcoRI and NotI. The expression plasmid for lGlcAT-P-AAA (pEF-BOS/lGlcAT-P-AAA) was constructed using QuikChange Lightning site-directed mutagenesis kits (Stratagene, La Jolla, CA) according to the manufacturer's protocol employing the primers listed below, with pEF-BOS/lGlcAT-P being used as a template. GlcAT-P-Fc (P-long-Fc, P-short-Fc, and P-AAA-Fc) expression plasmids were constructed as follows. A fragment was amplified by PCR using pEF-BOS/lGlcAT-P, pEF-BOS/sGlcAT-P, or pEF-BOS/lGlcAT-P-AAA as a template with the primers listed below to create a 3′-SpeI site. After the resulting fragment had been digested with SpeI, it was ligated to pEF-Fc, which had been double-digested with EcoRV and SpeI. The G-N13-GlcAT-P expression plasmid was constructed as follows. A fragment was amplified by PCR using pEF-BOS/lGlcAT-P as a template with the primers listed below to create a 3′-NotI site. After the fragment had been digested with NotI, it was phosphorylated with polynucleotide kinase. An annealed oligonucleotide corresponding to human B4GalT-I N-terminal 13 amino acids with a 5′-EcoRI stub was prepared using the synthetic oligonucleotides listed below. These two fragments were simultaneously ligated to pEF1/V5-HisA, which had been double-digested with EcoRI and NotI. The expression plasmid for G-N13AA-GlcAT-P was constructed using QuikChange Lightning site-directed mutagenesis kits employing the primers listed below, with pEF-1/V5-HisA/G-N13-GlcAT-P being used as a template. cDNA of the mouse PST (ST8Sia-IV)-coding sequence was amplified by PCR with the primers listed below using reverse-transcribed mouse brain total RNA as a template to create 5′-HindIII and 3′-XbaI sites. The fragment was ligated to p3×FLAG-CMV-14 (Sigma), which had been double-digested with the same enzymes. Construction of the P-N13-PST and G-N13-PST expression plasmids was performed as follows. A fragment was amplified by PCR using the PST expression construct as a template with the primers listed below to create a 3′-XbaI site. After the fragment had been digested with XbaI, it was phosphorylated with polynucleotide kinase. An annealed oligonucleotide corresponding to the lGlcAT-P N-terminal 13 amino acids or those from human B4GalT-I with a 5′-HindIII stub was prepared using the synthetic oligonucleotides listed below. These two fragments were simultaneously ligated to p3×FLAG-CMV-14, which had been double-digested with HindIII and XbaI.

Primers and Oligonucleotides—Primers and nucleotides were listed as follows: lGlcAT-PΔstem for the longer fragment, TCCGACACGCTGCCCACCAT and TGAGCGGCCGCT-CAGATCTCCACCGAGGGGT (primer 1), for the shorter

fragment, CATGAATTCGGACTCTGCAAACCTGCTGC and GCTCTGGTGCCAGACGGTGA; lGlcAT-P-AAA, GGCGCAGCCAGCCTTGGAGATGCCGGCGGCAGCGGACATCCTCGCG and the complementary sequence; P-long-Fc and P-AAA-Fc, GCCACCATGGGTAATGAGGAGCTGTG and CCGACTAGTACTCACCCACCACCTCCACGATGTCAC (primer 2); P-short-Fc, GCCACCATGCCGAAGAGAAGGGACAT and primer 2; G-N13-GlcAT-P primers, ATGCCGAAGAGAAGGGACAT and primer 1; G-N13-GlcAT-P oligonucleotides, AATTGCCACCATGAGGCTTCGGGAGCCGCTCCTGAGCGGCAGCGCCGCG and CGCGGCGCTGCCGCTCAGGAGCGGCTCCCGAAGCCTCATGGTGGC (oligonucleotide 1); G-N13AA-GlcAT-P, GGTGGAATTGCCACCATGGCGCTTGCGGAGCCGCTCCTGAGCGGC and the complementary sequence; PST, TTTAAGCTTCACCCAAGATGCGCTCAATT and TGTTCTAGATTGCTTCATGCACTTTCCTG (primer 3); P-N13-PST primers, ATGCGCTCAATTAGAAAACG and primer 3, oligonucleotides, AGCTGCCACCATGGGTAATGAGGAGCTGTGGGCGCAGCCAGCCTTGGAG and CTCCAAGGCTGGCTGCGCCCACAGCTCCTCATTACCCATGGTGGC; G-N13-PST oligonucleotides, AGCTGCCACCATGAGGCTTCGGGAGCCGCTCCTGAGCGGCAGCGCCGCG and oligonucleotide 1. Underlining indicates restriction sites.

Cell Culture and Transfection—Neuro2A cells were cultured in minimum Eagle's medium supplemented with Earle's salts, nonessential amino acids, and 10% fetal bovine serum. For transfection, cells, plated on 6-cm (or 10-cm) tissue culture dishes, were transfected with 1 μg (4 μg in the case of 10-cm dishes) of each expression vector using FUGENE6 transfection reagent (Roche Applied Science) according to the manufacturer's protocol. After a 6-h incubation, the culture medium was replaced with serum-free Opti-MEM I (Invitrogen) in the case of analyzing proteins secreted into the medium. Cells and media were collected at 24 h post-transfection. The collected culture medium was ultracentrifuged at 105,000 $\times$ *g* for 20 min to exclude contamination by cellular membranous components, and proteins secreted into the culture medium were precipitated with ethanol and then solubilized in Laemmli sample buffer.

SDS-PAGE and Western Blotting—SDS-PAGE and Western blotting were carried out as described previously (8). In the case of PSA detection, 2% BSA in PBS containing 0.05% Tween 20 was used for blocking and antibody dilution. For the other antibodies, 5% skim milk in PBS containing 0.05% Tween 20 was used. Protein bands were detected with SuperSignal West Pico (Pierce) using a Luminoimage Analyzer LAS-3000 (Fuji Film, Tokyo, Japan).

N-Glycosidase F Digestion—Proteins (50 μg) were denatured with PBS containing 0.5% SDS, 1% 2-mercaptoethanol, and 4 mM EDTA. After the solution had been diluted with 4 volumes of PBS containing Nonidet P-40 (final concentration, 0.5%), 5 units of *N*-glycosidase F (Roche Applied Science) was added, followed by incubation for 12 h at 37 °C.

Immunofluorescence Staining—At 24 h post-transfection, cells were washed with PBS, fixed with ice-cold methanol, and then incubated with primary antibodies followed by incubation with Alexa Fluor-conjugated secondary antibodies. For DsRed2 detection, cells were fixed at 48 h post-transfection with 4% paraformaldehyde in PBS and blocked with 3% bovine serum albumin in PBS containing 0.1% Triton X-100. Cells were visualized with a Fluoview laser confocal microscope system (Olympus, Tokyo, Japan).

Glucuronyltransferase Assay—Glucuronyltransferase activity toward asialo-orosomucoid was measured as described previously (8). As an enzyme source, a Neuro2A cell lysate or concentrated conditioned medium was prepared. Neuro2A cells were plated on 10-cm culture dishes and then transfected with the expression plasmid, followed by medium replacement with Opti-MEM I after a 6-h incubation. Cells were collected at 48 h after transfection and lysed with 500 μl of Tris-buffered saline containing 1% Triton X-100 and a protease inhibitor mixture (Nacalai Tesque, Kyoto, Japan), and after centrifugation, the clarified lysate was used. The culture medium was ultracentrifuged, as described above, and then used after concentration to 500 μl with an Amicon Ultra centrifugal filter device (Millipore, Bedford, MA). 5 μl of each solution was used as an enzyme source.

Co-precipitation Experiment—We performed a co-precipitation experiment in which we referred to a method used in an *in vitro* binding experiment between Sar1 and immobilized cytoplasmic tail peptides of glycosyltransferases (16). Human recombinant full-length Sar1 protein fused to T7 tag at its N terminus was purchased from Abcam (Cambridge, MA). Neuro2A cells, plated on 6-cm culture dishes, were transfected with the expression plasmid encoding P-long-Fc, P-short-Fc, or P-AAA-Fc and then lysed with 300 μl of Tris-buffered saline containing 1% Triton X-100 and protease inhibitors. After centrifugation at 15,000 $\times$ *g* for 10 min, 1.2 μg of T7-tagged Sar1 was added to the supernatant, and then the mixture was incubated for 30 min at 4 °C. A fraction of the mixture was recovered for Western blotting, with Protein G-Sepharose TM4 Fast Flow being added to the rest of the mixture, followed by incubation for 2 h. The beads were precipitated and washed three times with an excess volume of the buffer (Tris-buffered saline containing 0.5% Triton X-100). Proteins bound to the beads were eluted by boiling in Laemmli sample buffer.

RESULTS

Enhanced N-Glycan Glucuronylation by sGlcAT-P in Neuro2A Cells—Previously, we reported that GlcAT-P mRNA had two alternatively spliced variants in mouse, rat, and human brains (19, 20). As described above, a 16-bp insertion in mice or a 17-bp insertion in humans in the longer mRNA generated a new stop codon in-frame (Fig. 1*A*). As a result, longer mRNAs containing the insertion were translated to the short form proteins and *vice versa*, and the long and short enzymes differed in only the presence or absence of the N-terminal 13 amino acids (P-N13) in the cytoplasmic tail (Fig. 2*A*, lGlcAT-P and sGlcAT-P). We subcloned the rat cDNAs complementary to the two forms of mRNA using a rat brain cDNA pool and confirmed that a similar 16-bp insertion was also present in rats (Fig. 1*A*). To investigate the respective role of these two protein isoforms in cells, rat cDNAs (lGlcAT-P cDNA and sGlcAT-P cDNA complementary to the shorter and longer mRNA, respectively) were transfected into the neuroblastoma cell line Neuro2A.

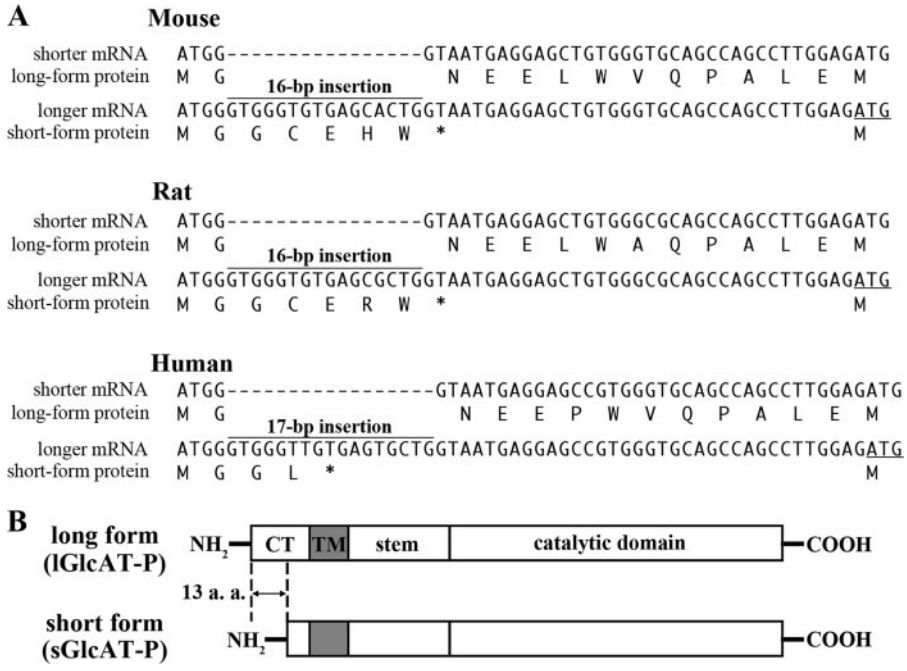

FIGURE 1. **Spliced variants of GlcAT-P.** *A*, cDNA sequences are shown around the initiation ATG complementary to the shorter and longer mRNA forms in mice, rats, and humans, and the corresponding amino acid sequence is depicted just *under* the respective cDNA sequence. The *underlined ATG* is a presumed initiation codon used in the longer mRNA. *B*, schematic diagram of lGlcAT-P and sGlcAT-P proteins. *CT*, cytoplasmic tail. *TM*, transmembrane domain.

After the cells had been harvested and lysed, they were treated with peptide:*N*-glycosidase F (PNGase F) to remove *N*-glycans to show the enzyme expression level clearly and then subjected to Western blotting (Fig. 2*B*). GP2 is an anti-GlcAT-P pAb against the GlcAT-P catalytic domain, which showed that almost equivalent amounts of the long and short isoforms were expressed (Fig. 2*B*, *top right*). In addition, only lGlcAT-P was detected with anti-P-N13, which is a rabbit pAb recognizing P-N13 (Fig. 2*B*, *bottom right panel*). To confirm that the second ATG was actually used as a translation initiation site when sGlcAT-P cDNA was transfected, we also subcloned GlcAT-P cDNA starting from the second ATG (Fig. 1*A*, *underlined*) integrated just downstream of an artificial Kozak sequence, GCCACC, into an expression vector, pEF1/V5-His A. The transfection of this construct into Neuro2A cells resulted in the same enzyme expression as in the case of sGlcAT-P cDNA regarding the molecular weight, biosynthetic activity, and subcellular localization (data not shown), indicating that in sGlcAT-P cDNA, including the 16-bp insertion, the second ATG was actually used as an initiation codon. Therefore, we employed sGlcAT-P cDNA in subsequent experiments. M6749 mAb, which exhibits similar epitope specificity to HNK-1 mAb, reacts with the HNK-1 epitope regardless of the terminal sulfate group (21). Since no band was detected for mock-transfected Neuro2A cells with M6749 mAb, Western blotting with this antibody allowed us to determine the amount of carbohydrate antigen synthesized by GlcAT-P expressed in the cells (Fig. 2*B*, *left*). As a result, a significantly higher expression level of the M6749 epitope on *N*-glycan was found in sGlcAT-P-expressing cells than in lGlcAT-P-expressing ones, despite the almost equivalent expression levels of the two enzymes. This indicates that sGlcAT-P has the ability to biosynthesize more abundant HNK-1 epitopes in cells than lGlcAT-P. It is possible that this higher epitope production was caused by the higher specific activity of sGlcAT-P, so we performed an *in vitro* activity assay using a Neuro2A cell lysate to compare the specific activities of the two GlcAT-P isoforms (Fig. 2*C*). Western blotting of the enzyme source extracts used for the activity assay (Fig. 2*C*, *right*) showed comparable enzyme expression and distinct product expression consistent with the results in Fig. 2*B*. However, the specific activities toward a glycoprotein acceptor substrate of the two isoforms were comparable (Fig. 2*C*, *left*), reflecting the enzyme expression levels. This excluded the possibility that the higher product biosynthesis in sGlcAT-P-expressing cells was due to its higher specific activity.

Subcellular Localization and Secretion of the Two GlcAT-P Isoforms—Next, we investigated the subcellular localization of the two GlcAT-P isoforms. Neuro2A cells expressing lGlcAT-P or sGlcAT-P were immunostained with GP2 pAb and anti-GM130 mAb (Golgi marker) (Fig. 3*A*). As a result, sGlcAT-P was found to show strict accumulation in the Golgi apparatus, whereas lGlcAT-P was localized mainly in the Golgi but partly in the ER (Figs. 3*A* and 4*B*), suggesting that some lGlcAT-P remained in the ER, probably due to slow export from the ER. The results were similar to the two isoforms of a sialyltransferase, ST6Gal-I (22). The two isoforms of this enzyme differ in only a single amino acid in the catalytic domain generated on RNA editing. The ST6Gal-I isoforms were differently localized in cells like those of GlcAT-P (23). ST6Gal-I is well known to be cleaved at its stem region and secreted extracellularly as a soluble form (24), and the secretion levels of the two isoforms were shown to significantly differ (23). Based on these reports, we investigated whether or not GlcAT-P was cleaved and secreted (Fig. 3*B*). As a result, two bands were detected for both lGlcAT-P- and sGlcAT-P-expressing cell media, and the cleavage and secretion level of sGlcAT-P were higher than those of lGlcAT-P. The *in vitro* activity assay also confirmed the higher secretion of sGlcAT-P (Fig. 3*C*) and indicated that the cleaved GlcAT-P was catalytically active with an intact catalytic domain. Since many secreted glycosyltransferases are known to be generated in cells through cleavage at their stem regions (25), a mutant lGlcAT-P lacking the major part of its stem region (lGlcAT-PΔstem) was expressed to determine whether or not the mutant enzyme was cleaved. As expected, no cleavage product derived from lGlcAT-PΔstem was detected in the culture medium (Fig. 3*D*), indicating that GlcAT-P was cleaved at its stem region like other glycosyltransferases.

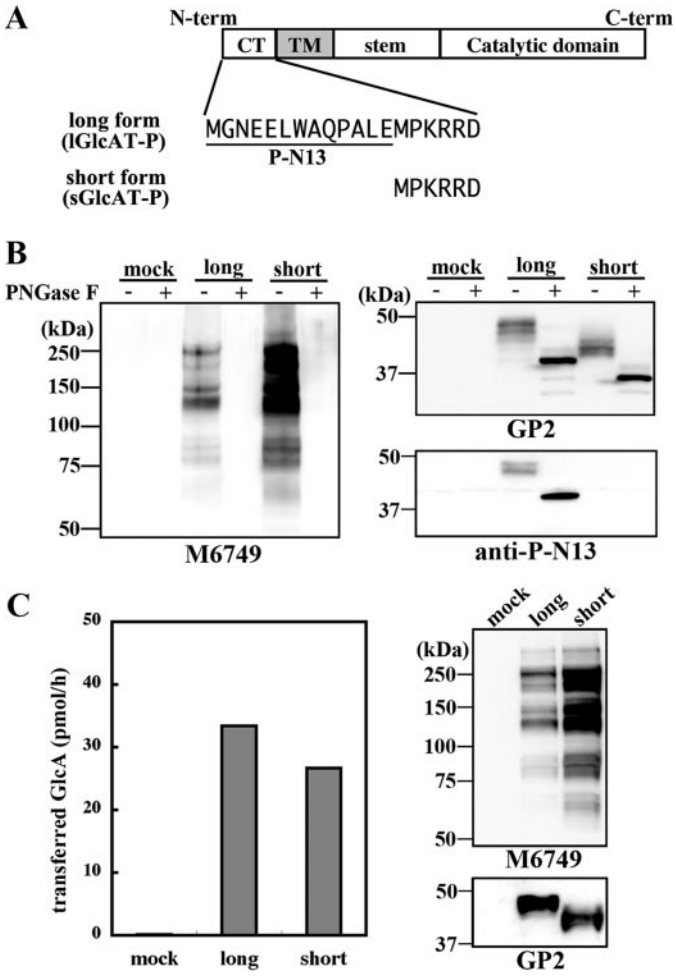

FIGURE 2. **Biosynthetic and *in vitro* glucuronylation activities of the two isoforms of rat GlcAT-P.** *A*, the two isoforms of GlcAT-P (lGlcAT-P and sGlcAT-P) differ in only the additional 13 amino acids (P-N13) in the N-terminal cytoplasmic tail. *B*, Neuro2A cells were transfected with the lGlcAT-P or sGlcAT-P expression plasmid or the empty vector (*mock*). Cells were lysed and treated with or without PNGase F and then subjected to Western blotting with M6749 mAb (*left*), GP2 (anti-GlcAT-P catalytic region) pAb (*top right*), or anti-P-N13 pAb (*lower right*). *C*, *in vitro* glucuronyltransferase activity toward a glycoprotein acceptor, asialo-orosomucoid, was measured. Mock treated-, lGlcAT-P-expressing, or sGlcAT-P-expressing Neuro2A cells were lysed and used as an enzyme source. The enzyme source solution was also subjected to Western blotting with M6749 mAb or GP2 pAb (*right*).

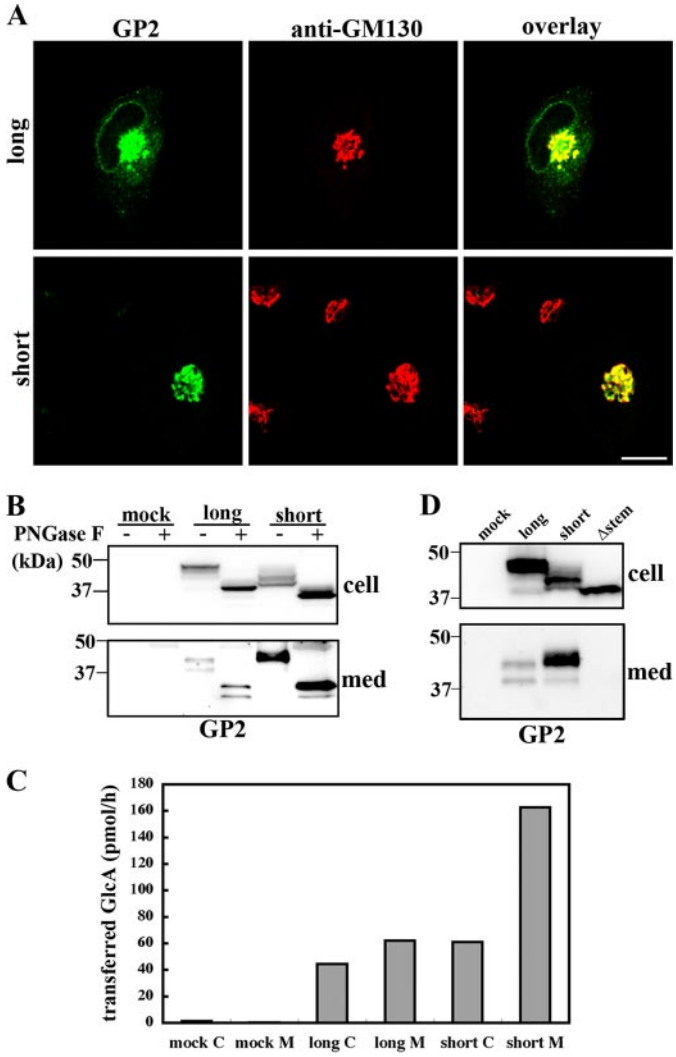

FIGURE 3. **Localization and secretion of the two isoforms of GlcAT-P.** *A*, Neuro2A cells expressing lGlcAT-P (*top*) or sGlcAT-P (*bottom*) were double-immunostained with GP2 pAb (*green*) and anti-GM130 mAb (*red*). The *right panels* show overlaid images. *Bar*, 10 μm. *B*, Neuro2A cells were transfected with the lGlcAT-P or sGlcAT-P expression plasmid or the empty vector (*mock*). Cellular proteins and proteins secreted into the culture medium (*med*) were treated with or without PNGase F and then subjected to Western blotting with GP2 pAb. *C*, *in vitro* glucuronyltransferase activity toward asialo-orosomucoid was measured. A mock-treated, lGlcAT-P-expressing, or sGlcAT-P-expressing Neuro2A cell lysate (*C*) or concentrated culture medium (*M*) was used as an enzyme source. Since the same volume of each enzyme source was used, specific activities in cell lysates and culture medium cannot be directly compared using the values. *D*, Neuro2A cells were transfected with the lGlcAT-P, sGlcAT-P, or lGlcAT-PΔstem expression plasmid or the empty vector (*mock*). Cell lysates and proteins secreted into the culture medium were Western blotted with GP2 pAb.

Dibasic Motif Essential for Golgi Localization and Intracellular Activity of GlcAT-P—As for the mechanism responsible for the distinct localization, secretion, and intracellular activity of the two isoforms of GlcAT-P, we investigated the role of a dibasic motif of glycosyltransferase in its transport. It was reported that some glycosyltransferases have a [K/R](*X*)[K/R] motif in their cytoplasmic tail proximal to the transmembrane border and that this motif was recognized by a small GTPase, Sar1, to transport glycosyltransferases from ER to the Golgi apparatus (16). They also showed that disruption of the motif caused the entrapment of glycosyltransferases, such as GalT2 or GalNAcT, in ER. GlcAT-P also has this motif in its cytoplasmic tail (Fig. 4*A*, KRR). If this motif of GlcAT-P is essential for its transport and localization, P-N13 of lGlcAT-P adjacent to this motif may affect GlcAT-P transport, leading to the distinct localization of the two isoforms. To determine the importance of this motif, a mutant lGlcAT-P lacking this motif (lGlcAT-P-AAA), in which the KRR sequence was substituted with AAA, was expressed (Fig. 4*A*). Immunostaining of the Neuro2A transfectant demonstrated that Golgi localization of lGlcAT-P-AAA was significantly disrupted, and the majority of the mutant was entrapped in ER (Fig. 4*B*), indicating a fundamental role of this motif in GlcAT-P. In addition, the disrupted localization of GlcAT-P led to a significantly low expression of the M6749 epitope compared with the wild-type enzyme (Fig. 4*C*, *left*), also confirming the necessity of the motif for GlcAT-P to serve as a functional glycosyltransferase. It was noticeable that lGlcAT-P-AAA was barely secreted (Fig. 4*C*, *right*), implying that the

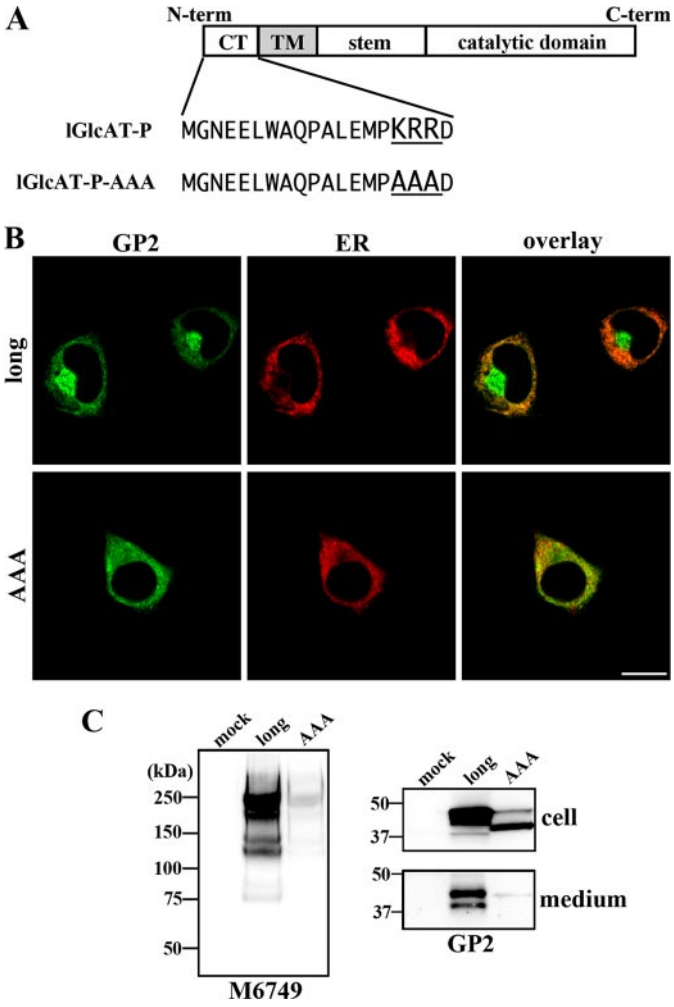

FIGURE 4. **Disruption of Golgi localization and intracellular activity of a mutant GlcAT-P lacking the dibasic motif.** *A*, in the cytoplasmic tail of GlcAT-P, a dibasic motif (KRR) exists. lGlcAT-P-AAA is a mutant lGlcAT-P lacking this motif. *B*, Neuro2A cells were co-transfected with the lGlcAT-P or lGlcAT-P-AAA expression plasmid and with pDsRed2-ER (Clontech). Cells were immunostained with GP2 pAb (*green*), and ER was visualized (*red*). Overlaid images are shown (*right*). *Bar*, 10 μm. *C*, Neuro2A cells were transfected with the lGlcAT-P or lGlcAT-P-AAA expression plasmid or the empty vector (*mock*). Cell lysates were Western blotted with M6749 mAb (*left*), and cell lysates and secreted proteins were Western blotted with GP2 pAb (*right*).

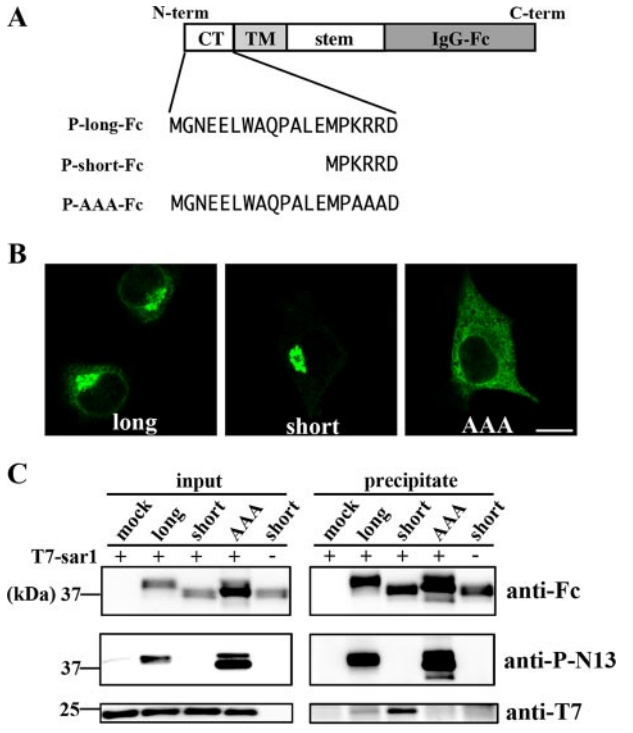

FIGURE 5. **Interaction between chimeric GlcAT-Ps and Sar1.** *A*, schematic diagrams of chimeric GlcAT-Ps are shown. The catalytic domains of these chimeras were replaced with the human IgG-Fc region. The N-terminal cytoplasmic tails of three chimeras, P-long-Fc, P-short-Fc, and P-AAA-Fc, correspond to those of full-length lGlcAT-P, sGlcAT-P, and lGlcAT-P-AAA, respectively. *B*, Neuro2A cells expressing P-long-Fc (*left*), P-short-Fc (*middle*), or P-AAA-Fc (*right*) were immunostained with anti-human IgG-Fc pAb. Note that the staining patterns shown here resemble those of the full-length enzymes (Figs. 2*A* and 3*B*). *Bar*, 10 μm. *C*, Neuro2A cells were transfected with the P-long-Fc, P-short-Fc, or P-AAA-Fc expression plasmid or the empty plasmid (mock). Cells were lysed and incubated with recombinant T7-tagged Sar1, followed by incubation with Protein G beads. The lysate mixture before precipitation (*left*) and the proteins precipitated with the beads (*right*) were Western blotted with anti-human IgG-Fc pAb (*top*), anti-P-N13 pAb (*middle*), or anti-T7 mAb (*bottom*).

cleavage of GlcAT-P occurred in the Golgi apparatus or in a subcellular compartment other than the ER.

Distinct Interaction of GlcAT-P Isoforms with the Small GTPase Sar1—Previously, the direct binding between Sar1 and the dibasic motif of a certain glycosyltransferase was shown (16). Therefore, we hypothesized that Sar1 also interacts with the KRR sequon in the GlcAT-P cytoplasmic tail, and P-N13 interferes with this interaction. To show this, we expressed a chimeric enzyme, GlcAT-P-Fc, whose catalytic domain was replaced with the human IgG-Fc region (Fig. 5*A*). As shown in Fig. 5*B*, these chimeric enzymes were localized in Neuro2A cells in almost the same way as the corresponding full-length GlcAT-Ps, indicating that from the N terminus to the stem region comprised a molecular determinant for the appropriate localization of this enzyme. Using these chimeric enzymes, the interaction with Sar1 was examined. Neuro2A cells expressing P-long-Fc, P-short-Fc, or P-AAA-Fc were lysed, and then T7-tagged Sar1 protein was added to the resultant lysate. After the precipitation of Fc-tagged enzymes with Protein G beads, the co-precipitated amount of T7-Sar1 was determined by Western blotting (Fig. 5*C*). Comparable amounts of the chimeric enzymes and an equivalent amount of T7-Sar1 existed in the mixture before precipitation, and anti-P-N13 blotting confirmed the expression of the chimeras with or without P-N13, as expected (Fig. 5*C*, *left*). In Fig. 5*C*, the *lower right panel* clearly shows that T7-Sar1 was co-precipitated with P-short-Fc much more than with P-long-Fc and that P-AAA-Fc, lacking the dibasic motif, was not co-precipitated with T7-Sar1. These results revealed that the dibasic motif in GlcAT-P was essential for Sar1 binding and that the existence of P-N13 weakened this interaction.

Chimeric PST (ST8Sia-IV) Bearing P-N13—To determine whether P-N13 had a similar effect on other glycosyltransferases, a chimeric enzyme, which was a polysialyltransferase, PST (ST8Sia-IV), fused with P-N13 at its N terminus, was expressed in Neuro2A cells (Fig. 6*A*). Polysialic acid (PSA), biosynthesized by PST (ST8Sia-IV) or STX (ST8Sia-II) (26, 27), is also a nervous system-specific carbohydrate, well known to be almost exclusively expressed on neural cell adhesion molecule,

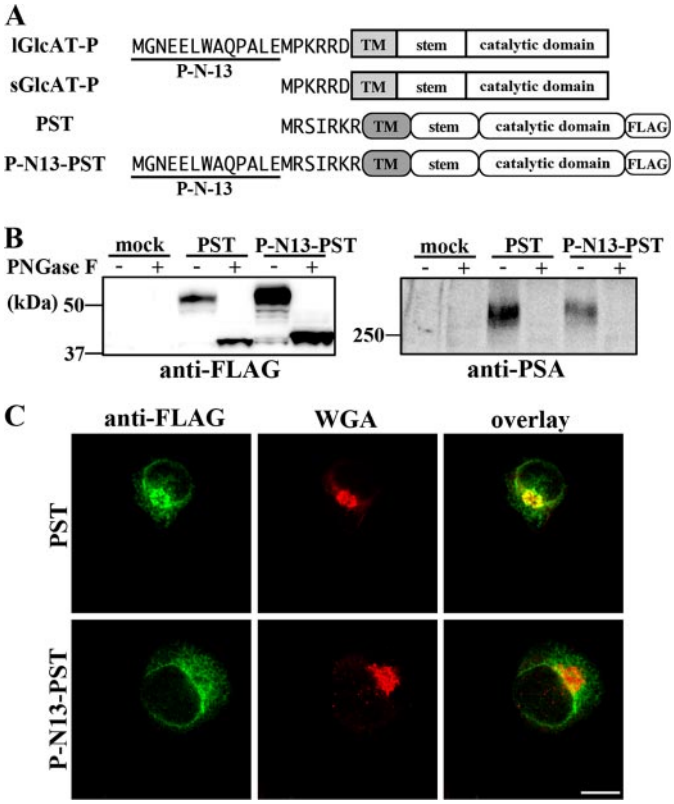

FIGURE 6. **Intracellular activity and localization of chimeric PST fused with P-N13.** *A*, schematic diagrams of 3×FLAG-tagged PST and chimeric PST are shown. The N-terminal cytoplasmic tails are depicted as the amino acid sequences. *B*, Neuro2A cells were transfected with the PST or P-N13-PST expression plasmid or the empty vector (*mock*). Cells were lysed and treated with or without PNGase F, followed by Western blotting with anti-FLAG mAb (*left*) or anti-PSA mAb (12E3) (*right*). *C*, Neuro2A cells expressing PST or P-N13-PST were co-stained with anti-FLAG mAb (*green*) and biotinylated wheat germ agglutinin lectin (*WGA*; Golgi marker; *red*). Overlaid images are shown (*right*). *Bar*, 10 μm.

and involved in synaptic plasticity (28). Since it was reported that Neuro2A cells expressed neural cell adhesion molecule endogenously (29), we are able to determine the level of PSA production by exogenously expressed PST in cells using Western blotting with anti-PSA antibodies. In addition, since PST has a dibasic motif in its cytoplasmic tail like GlcAT-P (Fig. 6*A*, RKR sequence), we can investigate the general roles of P-N13 in the regulation of glycosyltransferase localization and intracellular activity. C-terminal 3×FLAG-tagged PST or its chimera with P-N13 at the N terminus was expressed in Neuro2A cells, and then Western blotting with anti-FLAG or anti-PSA antibodies was performed (Fig. 6*B*). As shown in Fig. 6*B* (*right*), Neuro2A cells hardly expressed PSA endogenously, and the overexpression of PST produced PSA on *N*-glycans. The biosynthetic level of PSA was lower in P-N13-PST-expressing cells than in wild-type PST-expressing cells despite the higher enzyme expression (Fig. 6*B*). Moreover, co-staining with anti-FLAG mAb and Golgi marker wheat germ agglutinin lectin (30) showed that PST was mainly localized in Golgi, whereas P-N13-PST was not (Fig. 6*C*). These results were consistent with the intracellular activity and localization of sGlcAT-P and lGlcAT-P shown in Figs. 2 and 3, suggesting that the action of P-N13 was not GlcAT-P-specific but could also apply to other glycosyltransferases.

Sequence-specific Role of P-N13—As just described, the attachment of P-N13 to PST had effects on its localization and biosynthetic activity, as in the case of GlcAT-P (Fig. 6). However, it was a possibility that any peptide of 13 amino acids in length was capable of having a similar effect. To examine this possibility, another set of 13 naturally occurring N-terminal amino acids derived from the longer B4GalT-I isoform (G-N13) was attached to PST and sGlcAT-P (Fig. 7*A*). Unlike P-N13-PST, G-N13-PST exhibited Golgi localization (Fig. 7*B*) and biosynthetic activity comparable with that of wild-type PST (Fig. 7*C*). These results suggested that the effects of P-N13 were sequence-specific. Moreover, G-N13-GlcAT-P showed tight Golgi localization similar to sGlcAT-P (Fig. 7*D*), a relatively higher intracellular activity than lGlcAT-P (Fig. 7*E*, *left*), and higher production of the cleaved secreted form (Fig. 7*E*, *bottom right*), resembling the sGlcAT-P features. However, G-N13 also has a dibasic motif near the N terminus (Fig. 7*A*, RLR sequence, indicated by *dots*), and it is possible that G-N13 itself has an ability to transport glycosyltransferase to the Golgi apparatus. We expressed a mutant G-N13-GlcAT-P lacking the dibasic motif near the N terminus (G-N13AA-GlcAT-P) and revealed that G-N13AA-GlcAT-P exhibited significantly higher enzymatic activity in cells than lGlcAT-P (supplemental Fig. 1), indicating that the contribution of the dibasic motif in G-N13 was considerably lower than the inherent motif near the transmembrane border. Judging from these results for G-N13-PST and G-N13-GlcAT-P, P-N13 plays a specific role in the intracellular behavior of glycosyltransferase.

DISCUSSION

In the present study, we demonstrated that the two isoforms of the HNK-1-sythesizing enzyme, GlcAT-P, differing in only the N-terminal cytoplasmic tail length, showed significantly distinct behavior, such as in localization, secretion, and HNK-1-producing activity in cells. Although the two isoforms were both functional in cells, as shown in Fig. 2*B*, their different intracellular activities could be a fine regulator of HNK-1 carbohydrate expression *in vivo*. These two isoforms were generated through alternative splicing in a conserved way in rodent and human brains (*i.e.* insertion right after the initiation codon generated an in-frame stop codon, resulting in the translation of the shorter enzyme, sGlcAT-P) (Fig. 1) (19, 20). Previously, we performed RT-PCR analysis using a brain RNA pool with primers in which the longer and shorter mRNAs were simultaneously and distinctly detected. As a result, although the precise ratios of the two mRNAs were not quantified, we revealed that lGlcAT-P is the major isoform in the mouse and rat, whereas sGlcAT-P is the major form in the human brain (19, 20). We do not know at present why the major isoforms are different among these species and whether or not the expression levels of the respective isoforms are regulated upon condition changes of cells, such as neural development and neurological disorder. However, if the proportion of the two isoforms of GlcAT-P changes under some cellular conditions, this probably results in a change in HNK-1 expression that can be explained by the different intracellular activities of the GlcAT-P isoforms.

Regarding the mechanism underlying the distinct localization of the two GlcAT-P isoforms, we focused on the ER exit

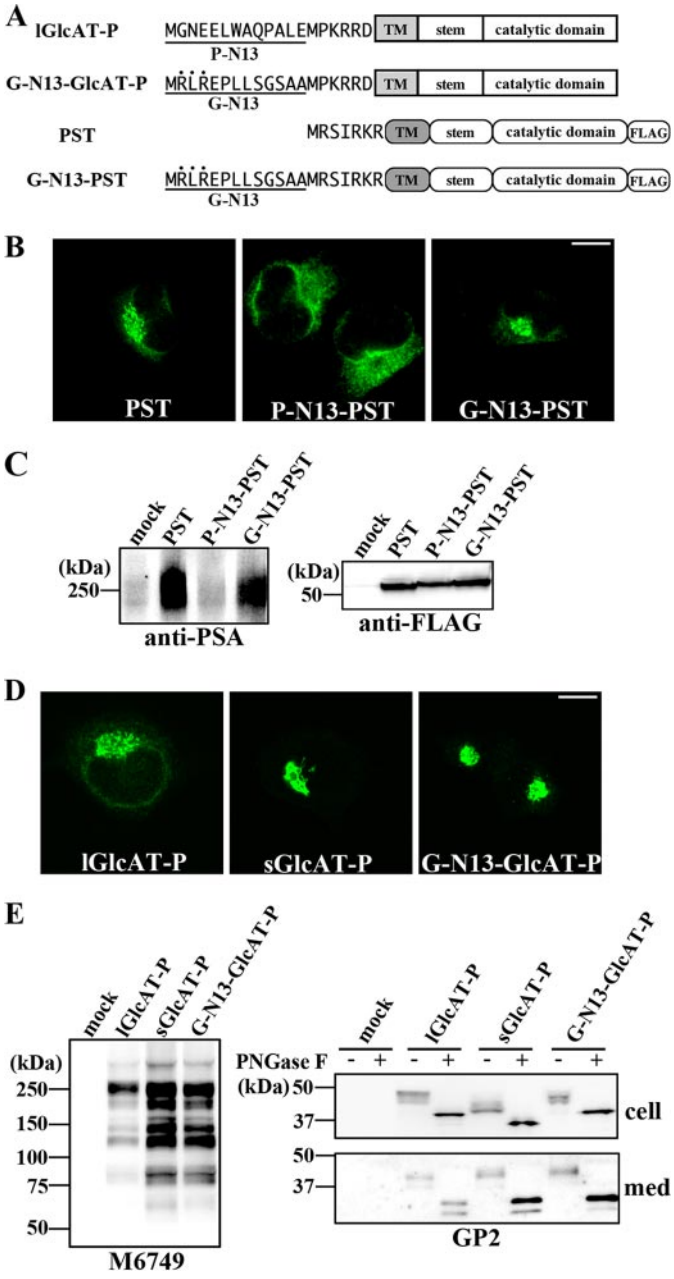

FIGURE 7. **Intracellular activities and localization of chimeric GlcAT-P and PST.** *A*, schematic diagrams of chimeric GlcAT-P and PST, which were fused with the N-terminal 13 amino acids from long form B4GalT-I (G-N13) at their N termini, are shown. The N-terminal cytoplasmic tails are depicted as the amino acid sequences. A dibasic motif in G-N13 near the N terminus is indicated by *dots*. *TM*, transmembrane domain. *B*, Neuro2A cells expressing wild-type PST, P-N13-PST, or G-N13-PST were immunostained with anti-FLAG mAb. Similar Golgi accumulation of PST and G-N13-PST was observed. *Bar*, 10 μm. *C*, Neuro2A cells were transfected with the PST, P-N13-PST, or G-N13-PST expression plasmid or the empty vector (*mock*). Cells were lysed and Western blotted with anti-PSA mAb (12E3) (*left*) or anti-FLAG mAb (*right*). *D*, Neuro2A cells expressing lGlcAT-P, sGlcAT-P, or G-N13-GlcAT-P were immunostained with GP2 pAb. sGlcAT-P and G-N13-GlcAT-P were similarly localized in the Golgi apparatus strictly. *Bar*, 10 μm. *E*, Neuro2A cells were transfected with the lGlcAT-P, sGlcAT-P, or G-N13-GlcAT-P expression plasmid or the empty vector (*mock*). Cells were lysed and Western blotted with M6749 mAb (*left*). Cellular proteins and proteins secreted into the medium (*med*) were treated with or without PNGase F, followed by Western blotting with GP2 pAb (*right*).

process mediated by the dibasic motif in the cytoplasmic tail. Consistent with a previous report (16), the dibasic motif in GlcAT-P near P-N13 was also essential for both Golgi localization and interaction with Sar1 (Figs. 4 and 5). In addition, we revealed, using a co-precipitation assay, that the interaction of sGlcAT-P with Sar1 was stronger than that of lGlcAT-P (Fig. 5*C*), probably because the existence of P-N13 interfered with this binding. Sar1 recruitment initiates the budding of COPII vesicles from ER (31), and COPII vesicles selectively incorporate and convey diverse cargoes, including glycosyltransferases from ER (32). In fact, the expression of a GTP-restricted or GDP-restricted form of Sar1 blocked the ER exit process, leading to the disruption of proper glycosyltransferase localization (33). Moreover, the direct binding of a cargo protein, such as viral glycoprotein VSV-G, to Sar1 promotes its efficient ER export (32). Therefore, the weaker interaction with Sar1 was considered to lead to the partial ER distribution of lGlcAT-P (Fig. 3*A*). On the other hand, as shown in Fig. 7, *D* and *E*, the attachment of another 13 amino acids (from human B4GalT-I) to sGlcAT-P caused neither ER entrapment nor an activity decrease. Further, P-N13, but not G-N13, had similar effects, such as a localization change and reduced activity, on another glycosyltransferase, PST (Figs. 6 and 7), which has a similar cytoplasmic tail with a dibasic motif to sGlcAT-P. These results refuted the idea that any peptide near the dibasic motif had an influence on glycosyltransferase localization and activity, rather suggesting a sequence-specific role of P-N13. However, the dibasic motif is also present in G-N13 near the N terminus (RLR sequence). Although this sequence might also be bound with Sar1 and serve to effectively convey G-N13-GlcAT-P and G-N13-PST from ER to the Golgi apparatus, Maccioni's group (16) demonstrated that the dibasic motif is most effective when located proximal to the transmembrane border, and they showed that the Golgi localization of SialT2, which has two dibasic motifs near the N terminus and the transmembrane region, was not affected by mutation of the first motif or by the deletion of 15 amino acids, including the first motif. Moreover, we demonstrated that the mutant G-N13-GlcAT-P lacking the motif near the N terminus (G-N13AA-GlcAT-P) showed similar distribution to G-N13-GlcAT-P and significantly higher intracellular activity than lGlcAT-P (supplemental Fig. 1). These findings suggested that the motif in G-N13 was ineffective in the case of G-N13-GlcAT-P and G-N13-PST. Based on these findings, we assumed that an unidentified protein specifically binds with P-N13 to cause these effects, but further experiments are required to explore this possibility.

We also found that the production of cleaved secreted sGlcAT-P was higher than that of lGlcAT-P (Fig. 3*B*) and that the cleavage occurred at the stem domain of this enzyme (Fig. 3*D*), as in the case of other glycosyltransferases. This is the first report that GlcAT-P is also cleavable and secreted, but the cleavage mechanism, including the responsible protease and cleavage site, is largely unknown. Although it is well known that some glycosyltransferases are cleaved and secreted into body fluids (34), the cleavage mechanisms and roles of the soluble enzymes remain to be clarified except for in the cases of ST6Gal-I and GnT-V (35, 36). As for GlcAT-P cleavage, we revealed that the entry of GlcAT-P into the Golgi apparatus was at least required because the disruption of GlcAT-P export from ER led to a significant decrease in GlcAT-P secretion (Fig. 4*C*). We also found that a soluble fraction as well as a membrane

fraction prepared from a mouse brain homogenate contained glucuronyltransferase activity *in vitro*, whereas those from GlcAT-P-deficient mice did not (data not shown), indicating that GlcAT-P was also cleaved and existed as a soluble enzyme *in vivo*. We are now trying to identify the cleaving protease(s) and to elucidate the function of extracellular soluble GlcAT-P.

As shown in Fig. 2*B*, sGlcAT-P exhibited significantly higher biosynthetic activity than lGlcAT-P in cells. Regarding the cause of this phenomenon, we consider that there are two possibilities. One is that a larger production of soluble enzymes from sGlcAT-P caused a higher expression of product glycans. In the case of ST6Gal-I, the enhanced production of soluble ST6Gal-I induced by the overexpression of BACE1, which is the protease responsible for its cleavage, led to greater sialylation of soluble acceptor glycoproteins without alteration of the sialylation of membrane-anchored acceptors (35). Another possibility is that the strict Golgi accumulation of sGlcAT-P is the main cause of the higher intracellular activity, since ER-distributed lGlcAT-P cannot serve as a functional enzyme because of the lack of an acceptor substrate with a complex type *N*-glycan. We think that the latter possibility is more plausible for the following reasons. Although soluble GlcAT-P may also be freely accessible to soluble acceptor glycoproteins in the Golgi lumen like soluble ST6Gal-I, our results showed that sGlcAT-P biosynthesized a significantly larger amount of glycan epitopes for both membrane-anchored (cellular) and soluble (extracellular) glycoproteins (Fig. 2*B* and data not shown). In addition, in our experiments, we could not detect cleaved soluble PST secreted into the culture medium, suggesting that the reduced activity of PST with the attachment of P-N13 was irrelevant concerning its cleavage and secretion. Rather, it was likely that the lower polysialylation by P-N13-PST was caused by its significant loss of Golgi distribution (Fig. 6). Overall, we considered that the increased secretion of sGlcAT-P was not the main cause of the enhanced activity but a consequence of the distribution change and that P-N13 influenced enzyme export from ER by hampering the interaction with Sar1, leading to activity regulation.

Various roles of the cytoplasmic tail of glycosyltransferases have gradually been uncovered, as described (see Introduction). However, we considered that the cytoplasmic tail of each glycosyltransferase has a distinct role, since each tail consists of amino acids markedly different in length and sequence. The dibasic motif in the cytoplasmic tail does not exist in all glycosyltransferases, and even GlcAT-S, the glycosyltransferase most highly homologous to GlcAT-P, does not have this motif. The mechanisms underlying the selective ER export of glycosyltransferases without the dibasic motif remain to be elucidated. Glycosyltransferase isoforms differing in the cytoplasmic tail have hardly been identified except for B4GalT-I. The B4GalT-I isoforms and GlcAT-Ps examined here showed the common feature that the longer form has an additional N-terminal 13 amino acids, and functional roles of G-N13 have been reported (*i.e.* in cell surface expression of the enzyme and cycling between *trans*-Golgi and *trans*-Golgi network) (14, 15). On the other hand, we revealed that P-N13 contained a different signal from that of B4GalT-I (*i.e.* one involved in the exit of the enzyme from the ER which eventually led to the change of the product glycan expression). Now we are searching for proteins binding to P-N13 and investigating whether and how the balance of the expression levels of the two GlcAT-P mRNAs is regulated. If we are successful, a novel molecular mechanism to regulate the specific glycan expression in the nervous system will be uncovered.

Acknowledgment—We thank Dr. K. Nakayama (Kyoto University) for valuable discussion.

REFERENCES

1. Ohtsubo, K., and Marth, J. D. (2006) *Cell* **126,** 855–867
2. Lowe, J. B., and Marth, J. D. (2003) *Annu. Rev. Biochem.* **72,** 643–691
3. Nieke, J., and Schachner, M. (1985) *Differentiation* **30,** 141–151
4. Terayama, K., Oka, S., Seiki, T., Miki, Y., Nakamura, A., Kozutsumi, Y., Takio, K., and Kawasaki, T. (1997) *Proc. Natl. Acad. Sci. U. S. A.* **94,** 6093–6098
5. Seiki, T., Oka, S., Terayama, K., Imiya, K., and Kawasaki, T. (1999) *Biochem. Biophys. Res. Commun.* **255,** 182–187
6. Bakker, H., Friedmann, I., Oka, S., Kawasaki, T., Nifant'ev, N., Schachner, M., and Mantei, N. (1997) *J. Biol. Chem.* **272,** 29942–29946
7. Yamamoto, S., Oka, S., Inoue, M., Shimuta, M., Manabe, T., Takahashi, H., Miyamoto, M., Asano, M., Sakagami, J., Sudo, K., Iwakura, Y., Ono, K., and Kawasaki, T. (2002) *J. Biol. Chem.* **277,** 27227–27231
8. Kizuka, Y., Matsui, T., Takematsu, H., Kozutsumi, Y., Kawasaki, T., and Oka, S. (2006) *J. Biol. Chem.* **281,** 13644–13651
9. de Graffenried, C. L., and Bertozzi, C. R. (2004) *Curr. Opin. Cell Biol.* **16,** 356–363
10. Breton, C., Mucha, J., and Jeanneau, C. (2001) *Biochimie* (*Paris*) **83,** 713–718
11. Opat, A. S., van Vliet, C., and Gleeson, P. A. (2001) *Biochimie* (*Paris*) **83,** 763–773
12. Uliana, A. S., Giraudo, C. G., and Maccioni, H. J. (2006) *Traffic* **7,** 604–612
13. Kakuda, S., Sato, Y., Tonoyama, Y., Oka, S., and Kawasaki, T. (2005) *Glycobiology* **15,** 203–210
14. Hathaway, H. J., Evans, S. C., Dubois, D. H., Foote, C. I., Elder, B. H., and Shur, B. D. (2003) *J. Cell Sci.* **116,** 4319–4330
15. Schaub, B. E., Berger, B., Berger, E. G., and Rohrer, J. (2006) *Mol. Biol. Cell* **17,** 5153–5162
16. Giraudo, C. G., and Maccioni, H. J. (2003) *Mol. Biol. Cell* **14,** 3753–3766
17. Schmitz, K. R., Liu, J., Li, S., Setty, T. G., Wood, C. S., Burd, C. G., and Ferguson, K. M. (2008) *Dev. Cell* **14,** 523–534
18. Tu, L., Tai, W. C., Chen, L., and Banfield, D. K. (2008) *Science* **321,** 404–407
19. Mitsumoto, Y., Oka, S., Sakuma, H., Inazawa, J., and Kawasaki, T. (2000) *Genomics* **65,** 166–173
20. Yamamoto, S., Oka, S., Saito-Ohara, F., Inazawa, J., and Kawasaki, T. (2002) *J. Biochem.* **131,** 337–347
21. Tagawa, H., Kizuka, Y., Ikeda, T., Itoh, S., Kawasaki, N., Kurihara, H., Onozato, M. L., Tojo, A., Sakai, T., Kawasaki, T., and Oka, S. (2005) *J. Biol. Chem.* **280,** 23876–23883
22. Ma, J., Qian, R., Rausa, F. M., and Colley, K. J. (1997) *J. Biol. Chem.* **272,** 672–679
23. Fenteany, F. H., and Colley, K. J. (2005) *J. Biol. Chem.* **280,** 5423–5429
24. Kitazume, S., Tachida, Y., Oka, R., Kotani, N., Ogawa, K., Suzuki, M., Dohmae, N., Takio, K., Saido, T. C., and Hashimoto, Y. (2003) *J. Biol. Chem.* **278,** 14865–14871
25. Paulson, J. C., and Colley, K. J. (1989) *J. Biol. Chem.* **264,** 17615–17618
26. Eckhardt, M., Muhlenhoff, M., Bethe, A., Koopman, J., Frosch, M., and Gerardy-Schahn, R. (1995) *Nature* **373,** 715–718
27. Kojima, N., Yoshida, Y., and Tsuji, S. (1995) *FEBS Lett.* **373,** 119–122
28. Weinhold, B., Seidenfaden, R., Rockle, I., Muhlenhoff, M., Schertzinger, F., Conzelmann, S., Marth, J. D., Gerardy-Schahn, R., and Hildebrandt, H. (2005) *J. Biol. Chem.* **280,** 42971–42977
29. Kojima, N., Tachida, Y., and Tsuji, S. (1997) *J. Biochem.* (*Tokyo*) **122,** 1265–1273

30. Virtanen, I., Ekblom, P., and Laurila, P. (1980) *J. Cell Biol.* **85,** 429–434
31. Barlowe, C., d'Enfert, C., and Schekman, R. (1993) *J. Biol. Chem.* **268,** 873–879
32. Antonny, B., and Schekman, R. (2001) *Curr. Opin. Cell Biol.* **13,** 438–443
33. Stroud, W. J., Jiang, S., Jack, G., and Storrie, B. (2003) *Traffic* **4,** 631–641
34. Gerber, A. C., Kozdrowski, I., Wyss, S. R., and Berger, E. G. (1979) *Eur. J. Biochem.* **93,** 453–460
35. Sugimoto, I., Futakawa, S., Oka, R., Ogawa, K., Marth, J. D., Miyoshi, E., Taniguchi, N., Hashimoto, Y., and Kitazume, S. (2007) *J. Biol. Chem.* **282,** 34896–34903
36. Nakahara, S., Saito, T., Kondo, N., Moriwaki, K., Noda, K., Ihara, S., Takahashi, M., Ide, Y., Gu, J., Inohara, H., Katayama, T., Tohyama, M., Kubo, T., Taniguchi, N., and Miyoshi, E. (2006) *FASEB J.* **20,** 2451–2459